

Preparation of CrIS Full Resolution Processing

Yong Chen¹

Yong Han², Denis Tremblay³, Likun Wang¹,
Xin Jin⁴, and Fuzhong Weng²

¹Earth System Science Interdisciplinary Center, University of Maryland, College Park, MD, 20740

²NOAA Center for Satellite Applications and Research, College Park, MD, 20740

³Science Data Processing Inc., Laurel, MD, 20723

⁴ERT, Laurel, MD, 20723

STAR JPSS Annual Science Team Meeting, May 12-16, 2014

Contents

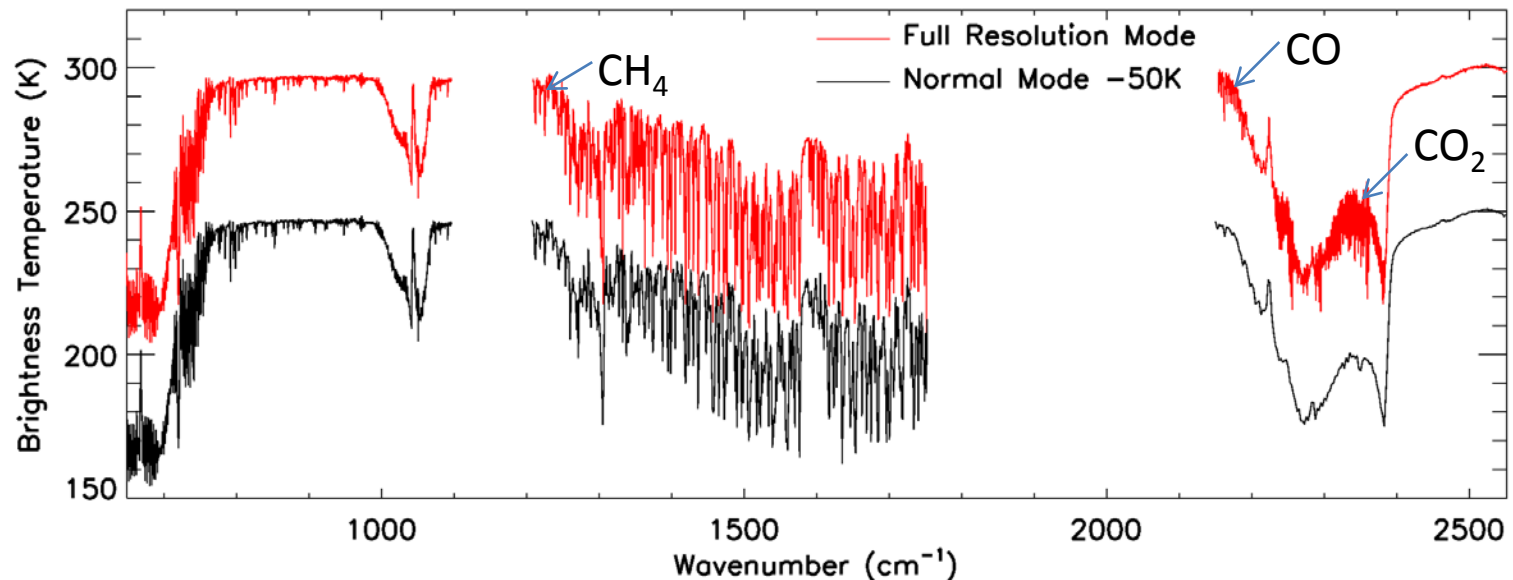
- ④ Prototype ADL to generate CrIS full resolution mode Sensor Data Records (SDR)
- ④ Comparison of different calibration approaches in ADL full resolution mode
- ④ Radiometric accuracy assessment
 - Difference between observation and forward model simulation
 - Double difference (DD) between CrIS and IASI
 - Simultaneous Nadir Overpass (SNO) between CrIS and IASI
- ④ Spectral accuracy assessment
 - Absolute spectral validation
 - Relative spectral validation
- ④ Summary

CrIS Normal Resolution and Full Resolution SDR

- CrIS can be operated in the full spectral resolution (FSR) mode with 0.625 cm^{-1} for all three bands, total 2211 channels, in addition to normal mode with 1305 channels
- NOAA will operate CrIS in FSR mode on December 2014 to improve the profile of H_2O , and the retrieval of atmospheric greenhouse gases CO , CO_2 , and CH_4

Red: Full resolution

Frequency Band	Spectral Range (cm^{-1})	Number of Channel (unapodized)	Spectral Resolution (cm^{-1})	Effective MPD (cm)
LWIR	650 to 1095	713* (717)	0.625	0.8
MWIR	1210 to 1750	433* (437)	1.25	0.4
		865* (869)	0.625	0.8
SWIR	2155 to 2550	159* (163)	2.5	0.2
		633* (637)	0.625	0.8



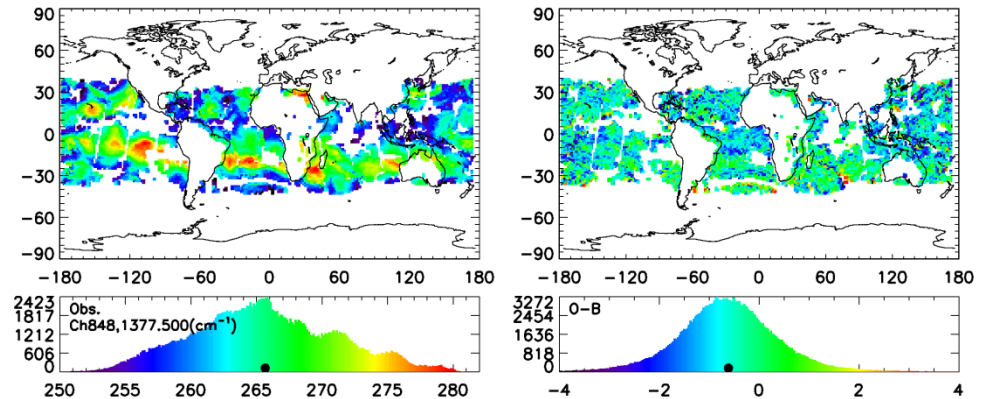
CrIS Normal Resolution SDR Generated from the FSR RDR

- Up to date, the FSR mode has been commanded three times in-orbit (02/23/2012, 03/12/2013, and 08/27/2013)
- CrIS normal mode SDR can be operationally generated from IDPS with the FSR RDR truncation modulus

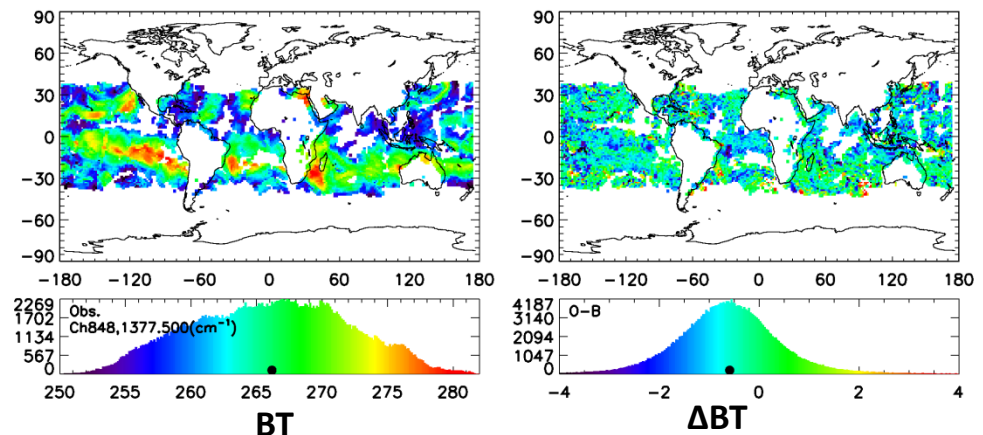
**CrIS normal mode SDR
Ch 848, 1377.5 cm^{-1} ,
water vapor channel**

- Results show that the SDR from FSR has similar features compared to SDR generated from low resolution RDR
- Both radiometric and spectral uncertainty are consistent with SDR generated from low resolution RDR

August 27, 2013, before FSR



August 27 and 28, 2013, FSR



Prototype ADL to Generate CrIS Full Resolution SDR

- A prototype ADL in full resolution model is developed based on ADL42&Mx8.3
- CrIS full resolution SDR are successfully generated offline using the three times in-orbit FSR RDR test data
- Different calibration approaches are implemented in the code in order to study the ringing effect observed in CrIS normal mode SDR and to support to select the best calibration algorithm for J1
- Code is modularized and flexible to run different calibration approaches, but need to be recompiled before running
- A lot of work still need to be done to make the code ready for delivery, such as calibration algorithm, Correction Matrix Operator (CMO), code interface, etc.
- Other models such as CCAST from UMBC/UW can also generate the CrIS full resolution SDR

Calibration Approaches

Item	Member	Calibration	CMO Principals	Calibration Order	
1	IDPS	$N = (SA_u^{-1} \cdot F_{s \rightarrow u} \cdot f_{ATBD}) \cdot \left\{ \frac{S_E - S_{SP}}{S_{ICT} - S_{SP}} \cdot ICT(T, u_{sensor^{*(1+\delta)}}) \right\}$	$SA_u^{-1} \cdot F_{s \rightarrow u}$		4th Best & Baseline
2	ADL/CSPP	$N = (SA_u^{-1} \cdot F_{s \rightarrow u} \cdot f_{ATBD}) \cdot \left\{ \frac{S_E - S_{SP}}{S_{ICT} - S_{SP}} \cdot ICT(T, u_{sensor^{*(1+\delta)}}) \right\}$			
3	Exelis (old)	$N = (SA_u^{-1} \cdot F_{s \rightarrow u} \cdot f_{ATBD}) \cdot \left\{ \frac{S_E - S_{SP}}{S_{ICT} - S_{SP}} \cdot f_{BH} \cdot [SA_u^{-1} \cdot F_{s \rightarrow u}]^{-1} \cdot ICT(T, u_{sensor}) \right\}$			
4	UMBC/UW** option A	$N = F_{s \rightarrow u} \cdot f \cdot SA_s^{-1} \cdot \left\{ f \cdot \frac{FIR^{-1} \cdot (S_E - S_{SP})}{FIR^{-1} \cdot (S_{ICT} - S_{SP})} \cdot ICT(T, u_{sensor_off_axis}) \right\}$	$F_{s \rightarrow u} \cdot SA_s^{-1}$	Calibration first, then CMO	2nd Best
5	CCAST Cal mode 1	$N = F_{s \rightarrow u} \cdot f \cdot SA_s^{-1} \cdot \left\{ \frac{FIR^{-1} \cdot (S_E - S_{SP})}{FIR^{-1} \cdot (S_{ICT} - S_{SP})} \cdot ICT(T, u_{sensor_off_axis}) \right\}$			
6	UMBC/UW** option B	$N = F_{s \rightarrow u} \cdot \left\{ ICT(T, u_{sensor}) \cdot f \cdot SA_s^{-1} \cdot \left\{ f \cdot \frac{FIR^{-1} \cdot (S_E - S_{SP})}{FIR^{-1} \cdot (S_{ICT} - S_{SP})} \right\} \right\}$			
7	CCAST Cal mode 2	$N = F_{s \rightarrow u} \cdot f \cdot \left\{ ICT(T, u_{sensor}) \cdot SA_s^{-1} \cdot \left[\text{Re} \left[\frac{FIR^{-1} \cdot (S_E - S_{SP})}{FIR^{-1} \cdot (S_{ICT} - S_{SP})} \right] \right] \right\}$			
8	LL(old)*	$N = \left\{ \frac{M \cdot (FIR^{-1} \cdot (S_E - S_{SP}))}{M \cdot (FIR^{-1} \cdot (S_{ICT} - S_{SP}))} \right\} \cdot ICT(T, u_{user})$		CMO first, then Calibration	Best
9	Proposed(1)	$N = F_{s \rightarrow u} \cdot f_{ATBD} \cdot \left\{ \frac{SA_s^{-1} \cdot (FIR^{-1} \cdot (S_E - S_{SP}))}{SA_s^{-1} \cdot (FIR^{-1} \cdot (S_{ICT} - S_{SP}))} \cdot ICT(T, u_{sensor}) \right\}$			
10	Proposed(2)	$N = ICT(T, u_{user}) \cdot \left\{ \frac{F_{s \rightarrow u} \cdot SA_s^{-1} \cdot f_{ATBD} \cdot (FIR^{-1} \cdot (S_E - S_{SP}))}{F_{s \rightarrow u} \cdot SA_s^{-1} \cdot f_{ATBD} \cdot (FIR^{-1} \cdot (S_{ICT} - S_{SP}))} \right\}$			
11	Exelis(new)	$N = \left\{ \frac{(SA_u^{-1} \cdot F_{s \rightarrow u} \cdot (S_E - S_{SP}))}{(SA_u^{-1} \cdot F_{s \rightarrow u} \cdot (S_{ICT} - S_{SP}))} \right\} \cdot ICT(T, u_{user})$	$SA_u^{-1} \cdot F_{s \rightarrow u}$		3rd Best

Most Desired Properties

From Dan and Joe 01/15/2014

(Preliminary Rankings of Calibration differences by Organization RevH - v2.xlsx)

Proposed 2 as Reference Calibration Approach

- Proposed 2 as reference calibration approach

$$N = ICT(T, u_{\text{user}}) \cdot \left\{ \frac{F_{s \rightarrow u} \cdot SA_s^{-1} \cdot f_{ATBD} \cdot (FIR^{-1} \cdot (S_E - S_{SP}))}{F_{s \rightarrow u} \cdot SA_s^{-1} \cdot f_{ATBD} \cdot (FIR^{-1} \cdot (S_{ICT} - S_{SP}))} \right\}$$

- SA matrix with delta approximation and sincq instead of sinc (Yong Han “correctionMatrix_withSincq_STAR.pptx” on 01/15/2014)

$$SA[k', k] \approx \int d\sigma' Sincq(2MPD(\sigma_{k'} - \sigma')) ILS(\sigma', \sigma_k)$$

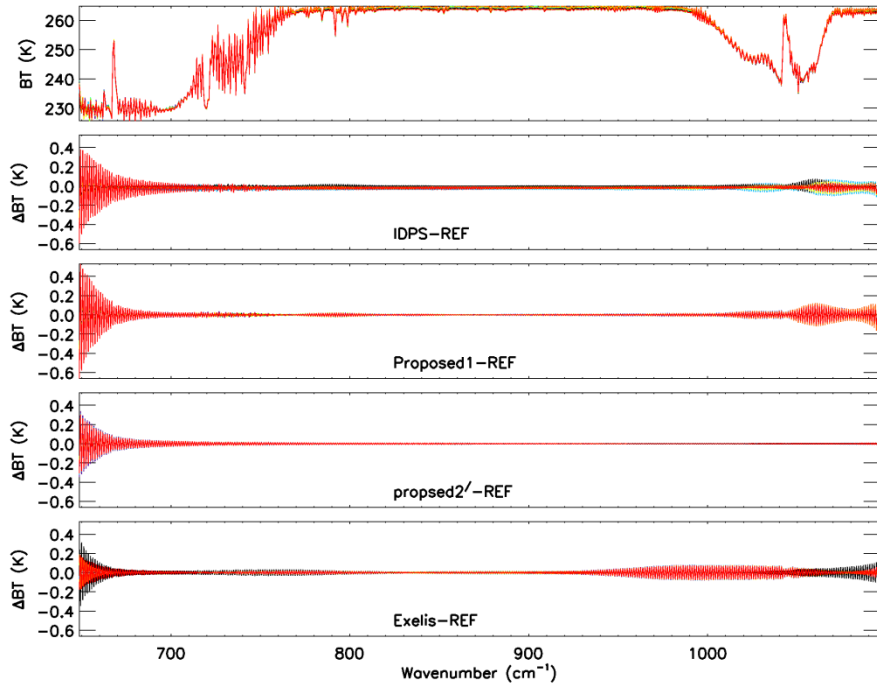
- Proposed 2': Interpolation to user grid using extended resampling method with larger N' instead of N
(Yong Han: “star_resampling_study.pdf” on 03/12/2014 and “Ring_reduction_withResampling_9Apr_2014.pdf” on 04/09/2014)

$$S_{k'} = \sum_{k=0}^{N-1} S_k \frac{1}{N'} \frac{\text{Sin}\left(\pi \frac{\sigma_{s,k'} - \sigma_{u,k}}{\Delta\sigma_u}\right)}{\text{Sin}\left(\pi \frac{\sigma_{s,k'} - \sigma_{u,k}}{N' \Delta\sigma_s}\right)}$$

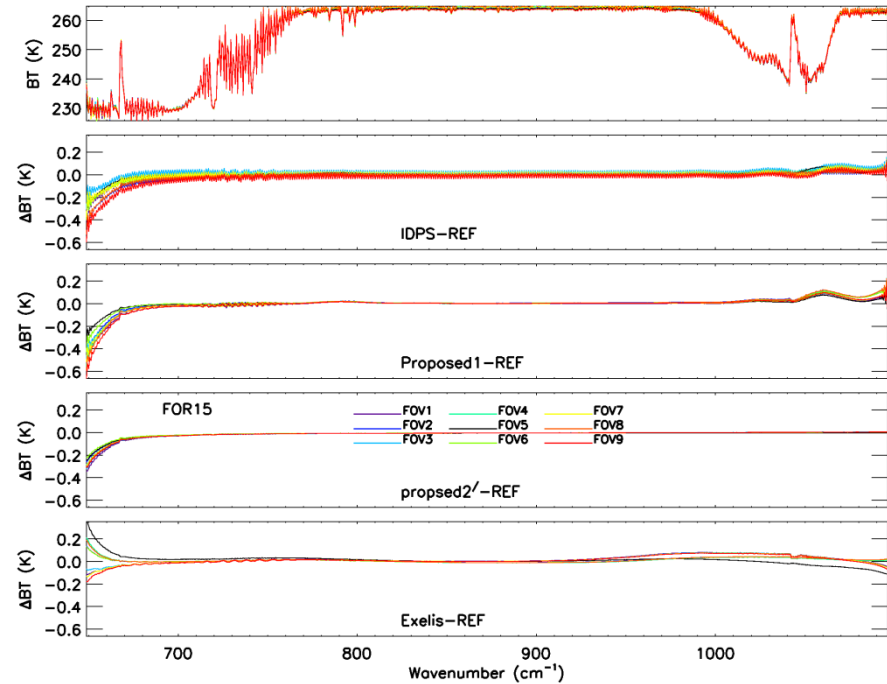
N' = DecimationFactor x N
N: Original spectrum binsize

Differences among Calibration Approaches for FOR15 and Band1

Ringing



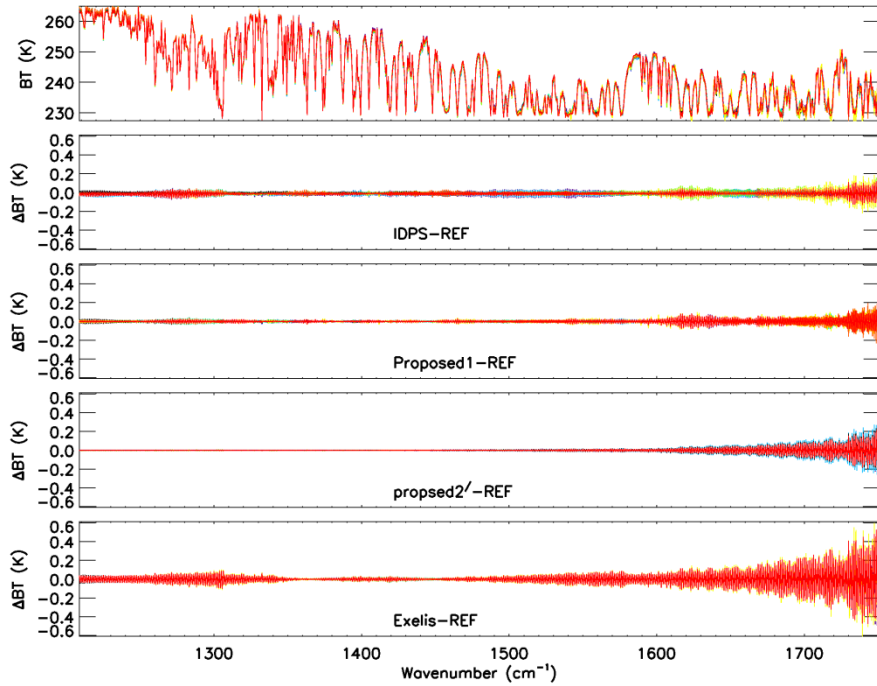
Envelope of Ringing



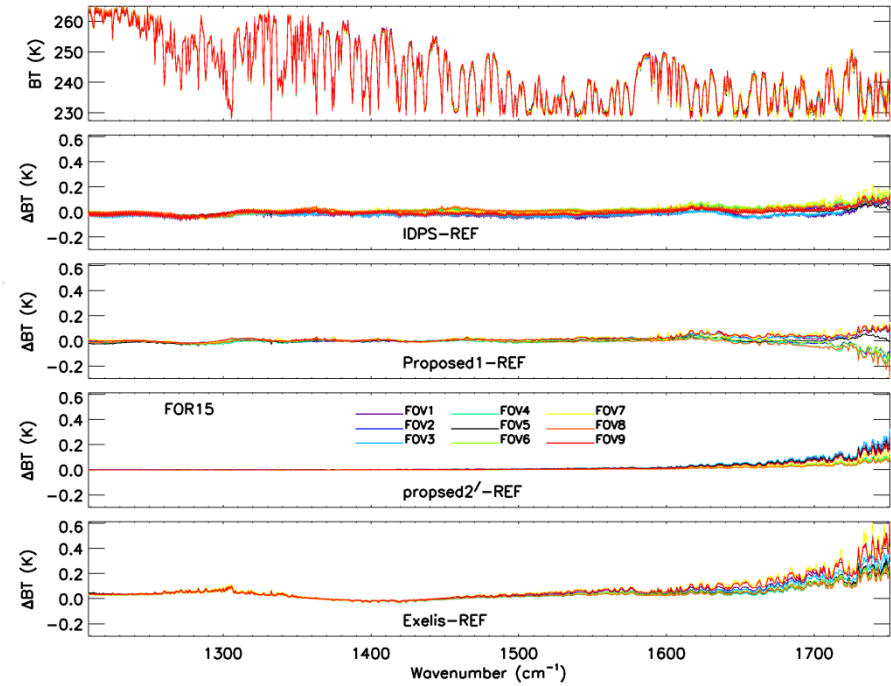
- The full resolution spectra were produced with a modified ADL code based on ADL42&Mx8.3 from full spectral resolution RDRs, collected when the CrIS was operated in the full spectral resolution mode on 08/27/2013
- Except for the proposed2' algorithm, all others use the same resampling method from ATBD
- Significant ringing among different approaches at the both band edges

Differences among Calibration Approaches for FOR15 and Band2

Ringing



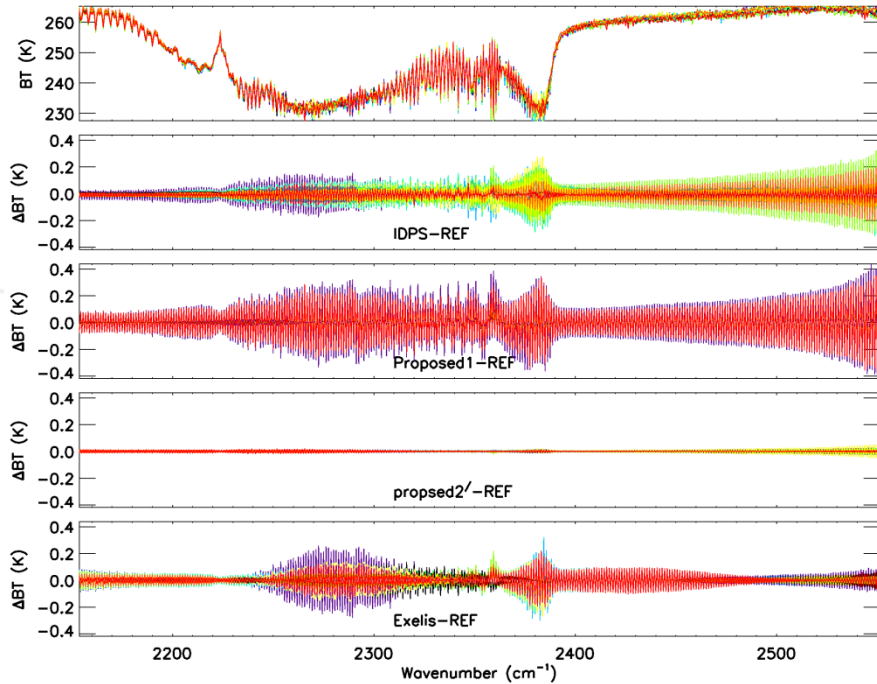
Envelope of Ringing



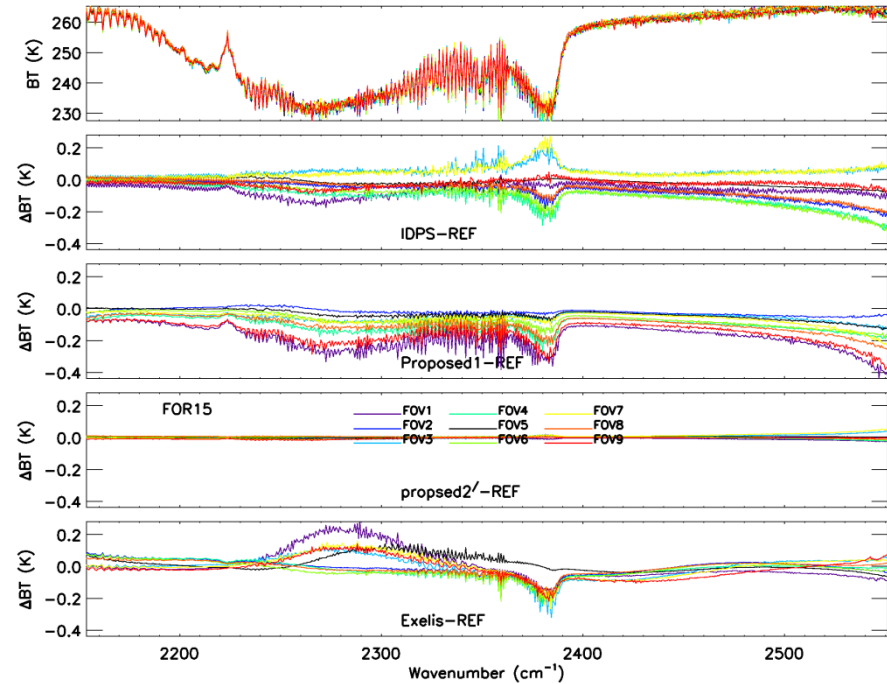
- Significant ringing among different approaches at the end of band edge

Differences among Calibration Approaches for FOR15 and Band3

Ringing



Envelope of Ringing



- Significant ringing at the band edge for IDPS and Proposed1
- Large ringing for the cold channels
- Which approach to use for the J1 algorithm? Need to define the truth reference, and consider the code interface changes and computing efficiency

CrIS Radiometric Assessment

- Validation of August 27-28, 2013 full spectral resolution data
- ADL42Mx8.3 used to generate full spectral resolution SDRs with updated non-linearity coefficients, ILS parameters, and sincq function for Correction Matrix Operator (CMO) for IDPS calibration approach.
- Assessment approach 1: Biases between CrIS observations and simulations using ECMWF analysis/forecast fields and forward model CRTM (Community Radiative Transfer Model)

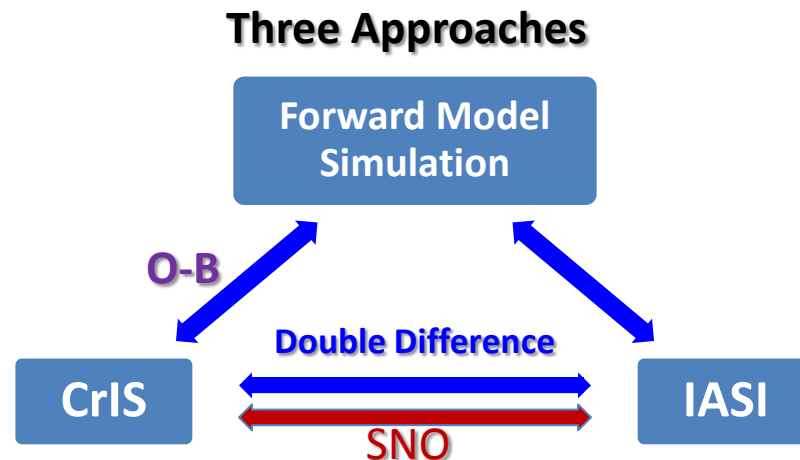
$$BIAS = \overline{(Obs - CRTM)}$$

- Assessment approach 2: Double difference between CrIS and IASI on MetOp-a/b (converted to CrIS) using CRTM simulation as a transfer tool

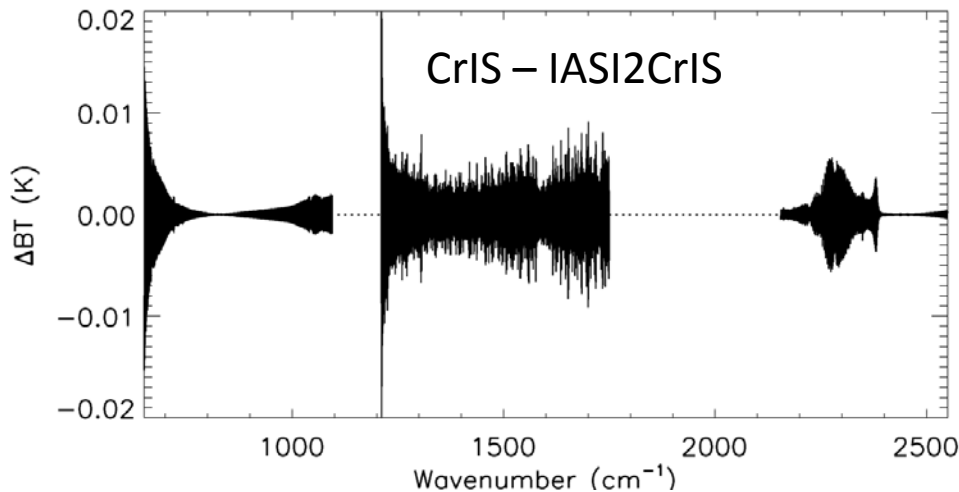
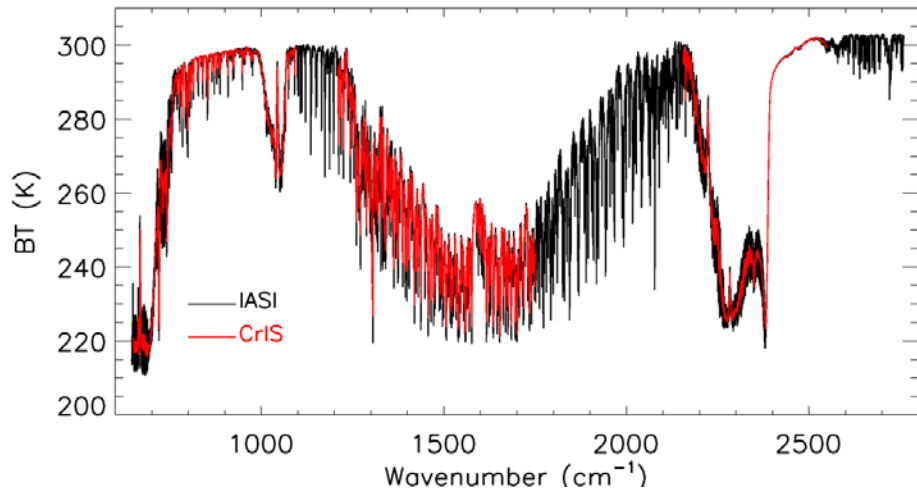
$$DD = \overline{(Obs - CRTM)_{CrIS}} - \overline{(Obs - CRTM)_{IASI2CrIS}}$$

- Assessment approach 3: SNO difference between CrIS and IASI converted to CrIS

$$BT_{diff} = BT_{CrIS} - BT_{IASI2CrIS}$$



Resample IASI to CrIS



IASI Observed Spectra

↓ FFT⁻¹

Inverse Fourier transform of the spectra to the interferogram space

↓ Apodization Function

- 1) De-Apodization with IASI SRF
- 2) Truncation to CrIS OPD
- 3) Apodization with CrIS SRF

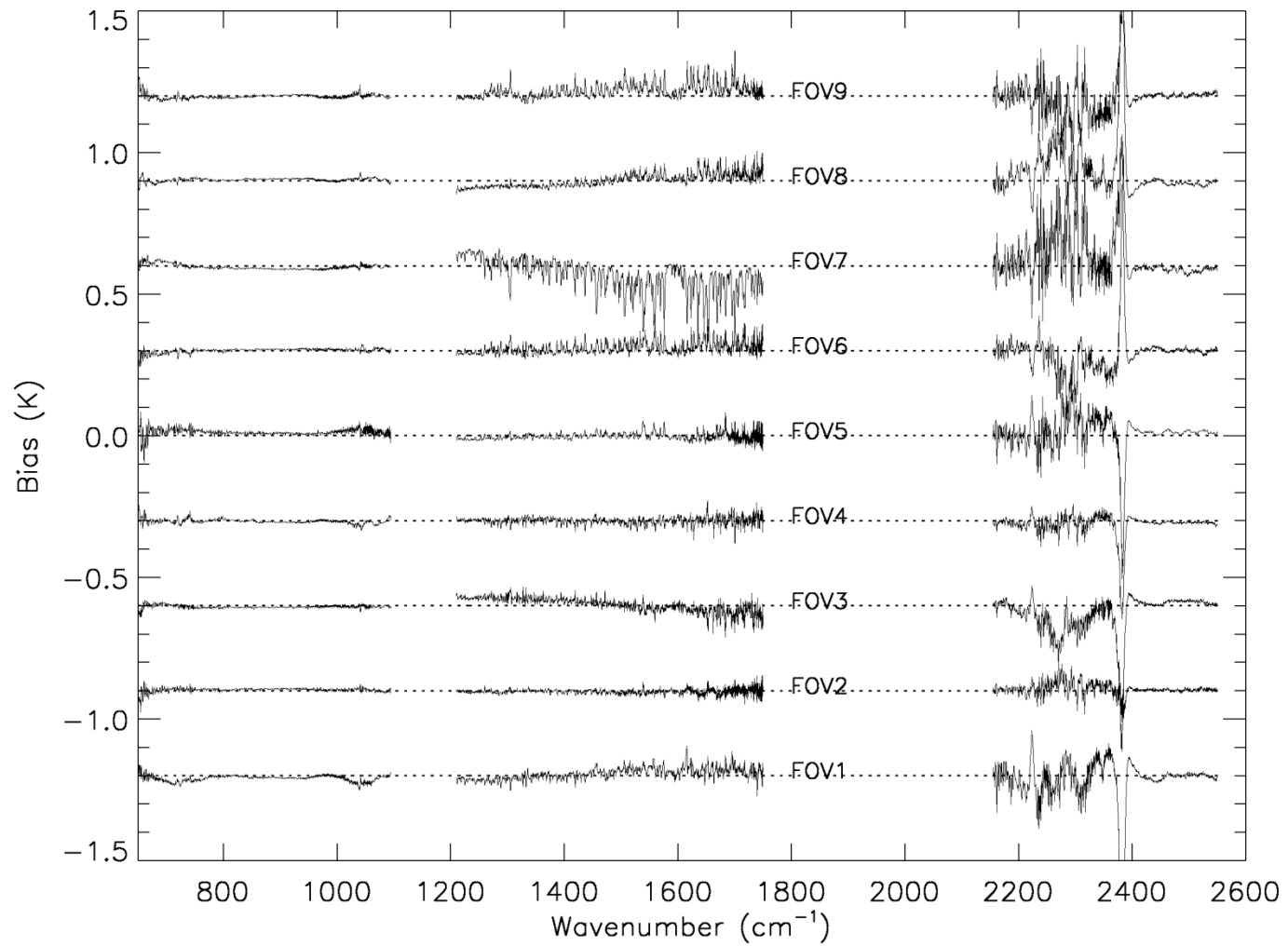
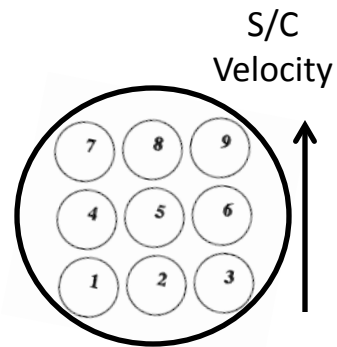
↓ FFT

Fourier transform of the products to spectra space, resampling the spectra on CrIS wavenumber basis.

- Resampling error from IASI to CrIS resolution is very small (less than 0.02 K) since IASI spectra cover CrIS spectra for all three bands

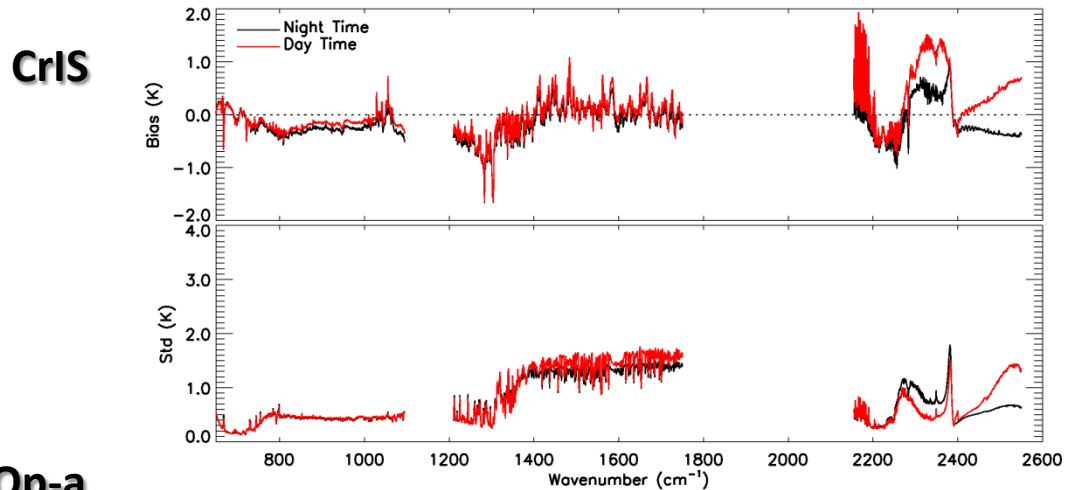
CrIS Nadir FOV-2-FOV Variability (FOR 15 and 16) for Clear Sky over Oceans

$$BIAS_{FOV_i} = \overline{(Obs - CRTM)_{FOV_i}} - \overline{(Obs - CRTM)_{all}}$$

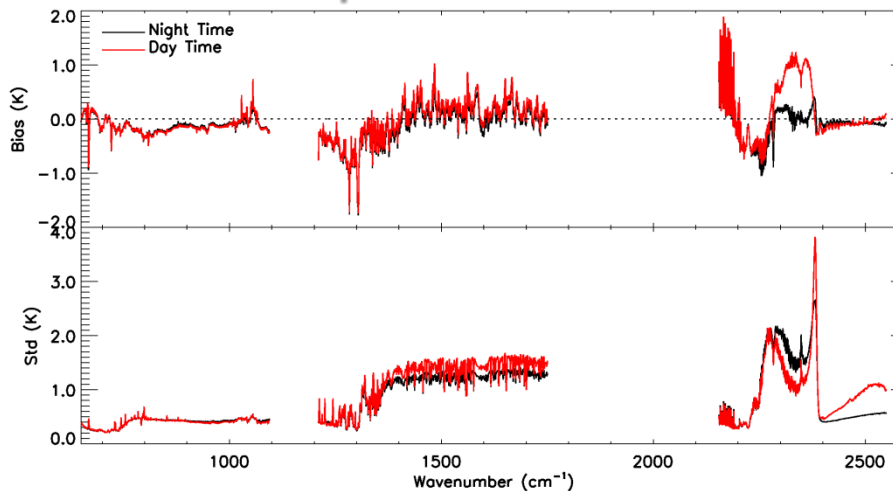


● **FOV-2-FOV variability is small, within ±0.3 K for all the channels**

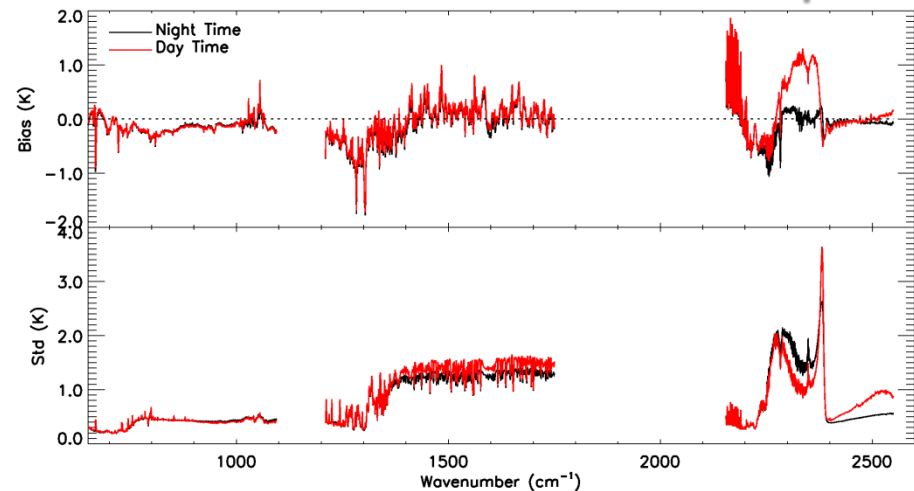
CrIS and IASI2CrIS NWP Biases: Clear Ocean Scenes



IASI2CrIS MetOp-a



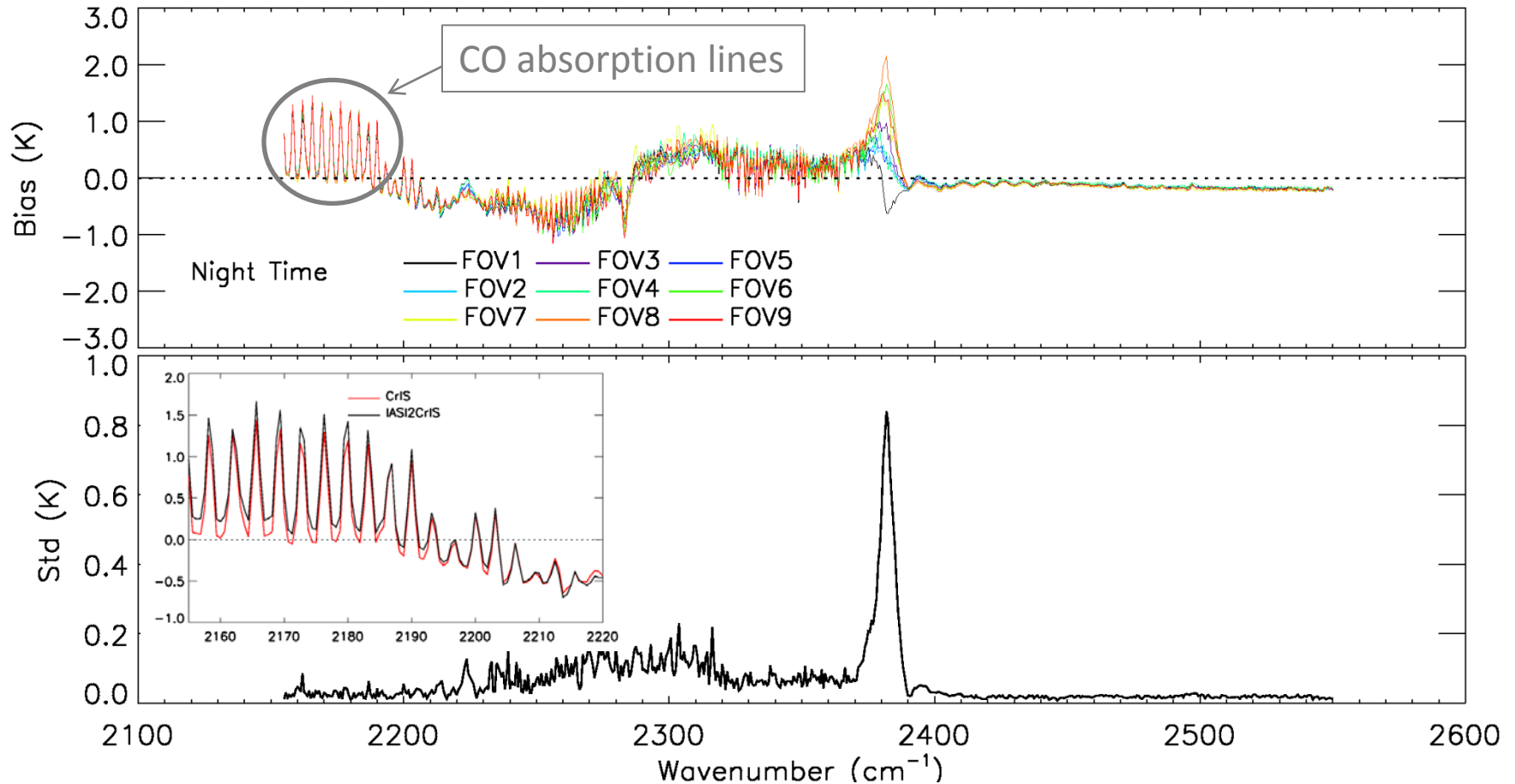
IASI2CrIS MetOp-b



- Good agreement between CrIS observation and simulation using ECMWF
- Very good agreement between CrIS and IASI
- Smaller standard deviation for CrIS than IASI in band 3

CrIS Nadir Bias for Shortwave

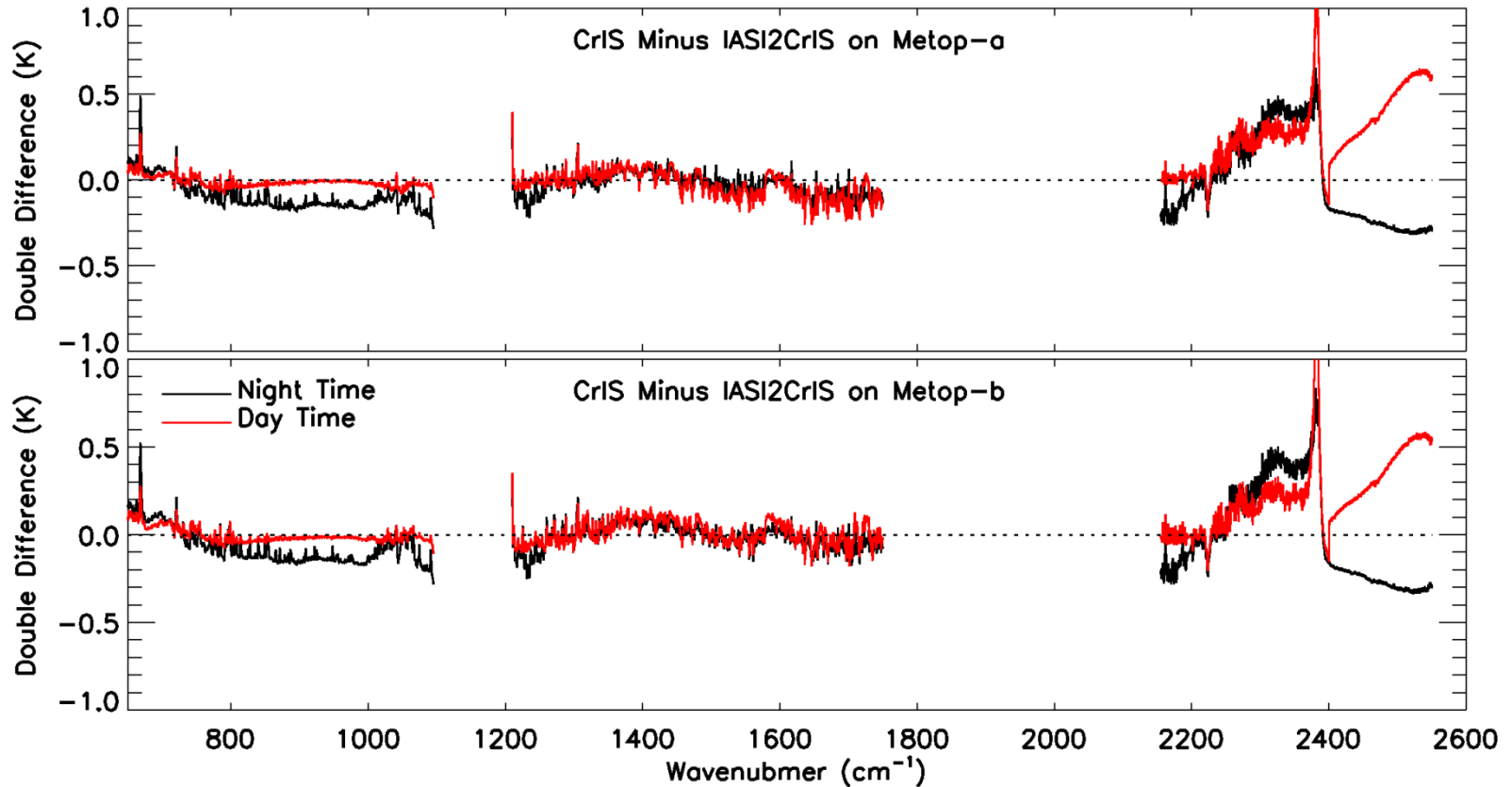
$$BIAS_{FOV_i} = \overline{(Obs - CRTM)}_{FOV_i}$$



- Good agreement between IASI and CrIS, better than bias with CRTM
- CO high bias errors due to CO default profile in CRTM
- CrIS and IASI window channels differ by 0.1 K due to diurnal variation in the SST

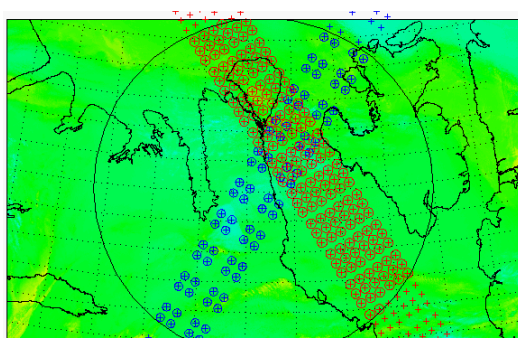
Double Difference between CrIS and IASI2CrIS

$$DD = \overline{(Obs - CRTM)_{CrIS}} - \overline{(Obs - CRTM)_{IASI2CrIS}}$$



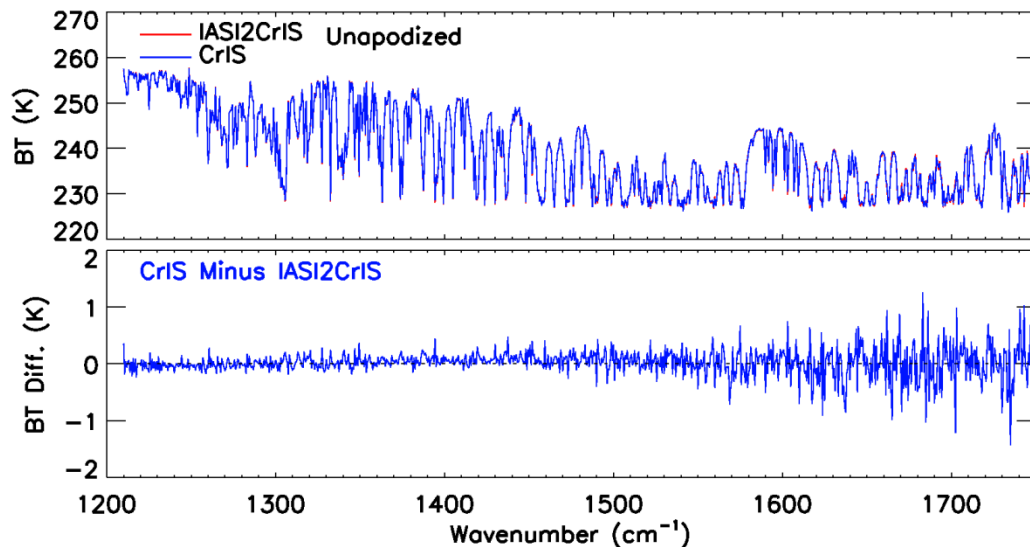
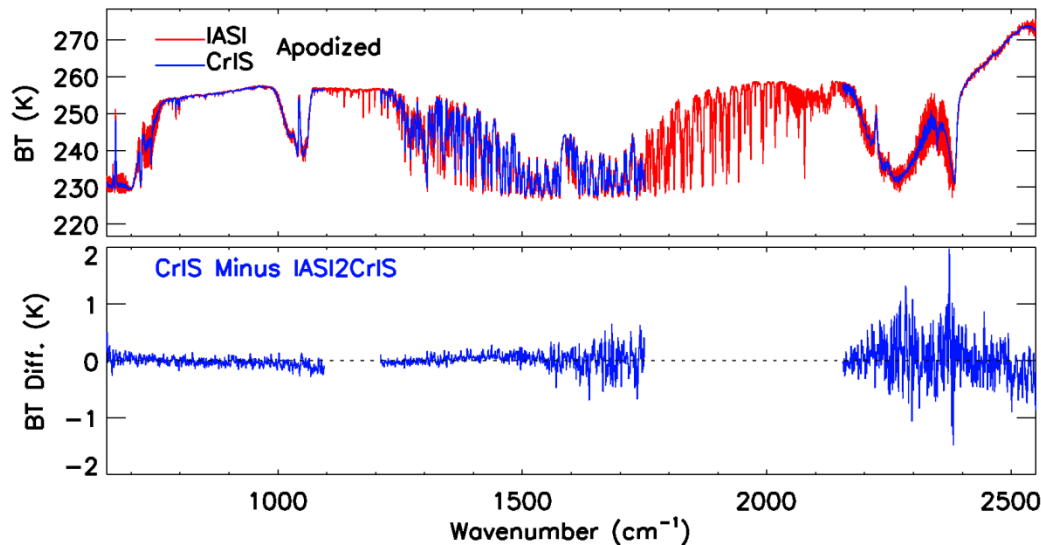
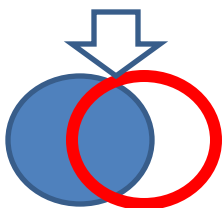
- Double difference between CrIS and IASI using CRTM simulations as transfer target are within ± 0.3 K for most of channels
- For $4.3 \mu\text{m}$ CO₂ strong absorption region, CrIS is warmer than IASI about 0.3-0.5 K
- CrIS and IASI window channels differ by 0.1 K due to diurnal variation in the SST

SNOs between CrIS and IASI



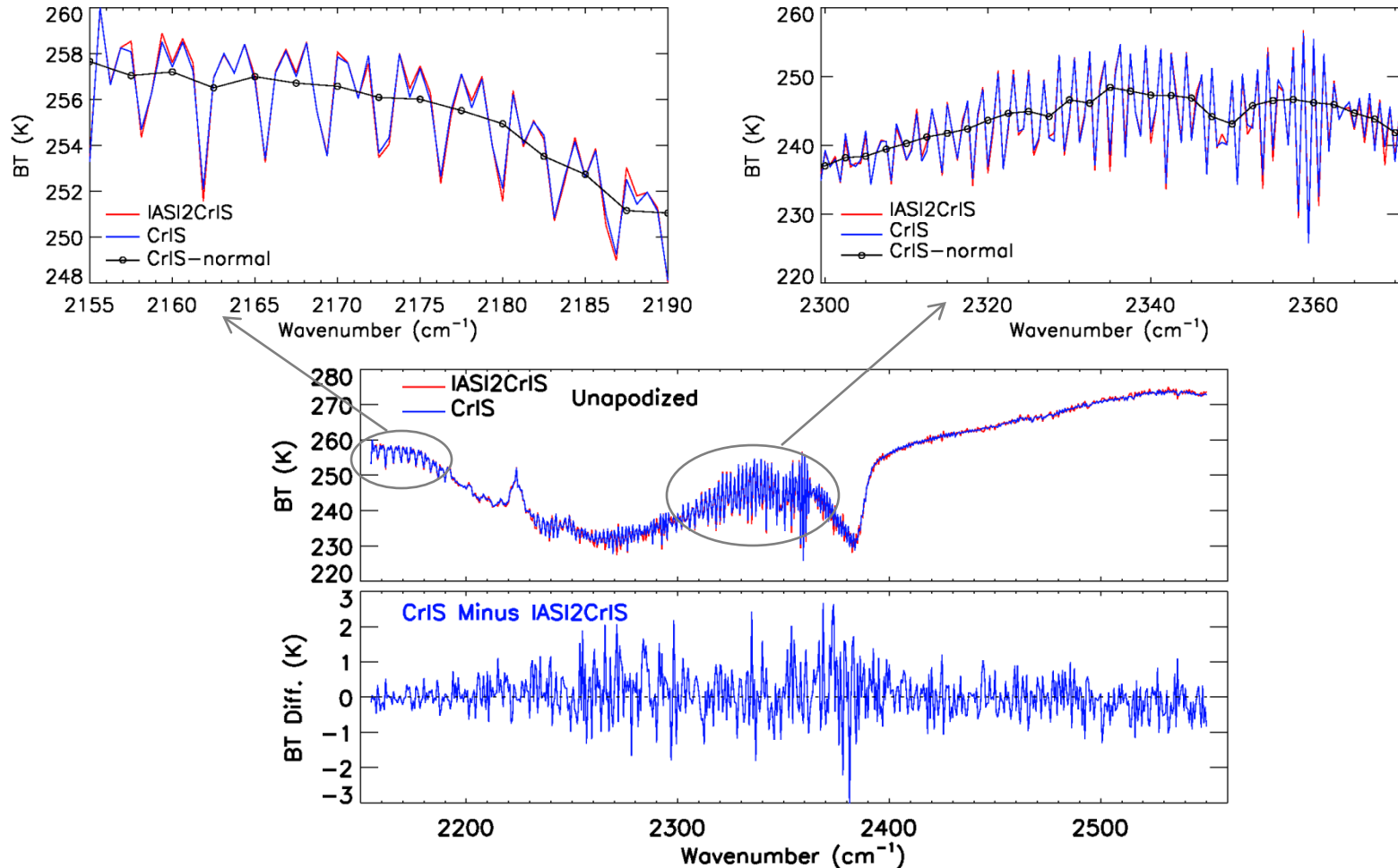
SNO Criteria

- Time difference:
 ≤ 120 seconds
- Pixel distance:
 $\leq (12+14)/4.0 \text{ km} = 6.5 \text{ km}$
- Zenith angle difference:
 $\text{ABS}(\cos(a1)/\cos(a2)-1) \leq 0.01$



- SNO agreement is very good for band 1. Also good for band 2, but larger BT difference toward the end of band edge
- Large BT differences in cold channels for band 3

SNOs between CrIS and IASI: Details



- Although there is large BT difference in band 3, line structures in CO and CO₂ region show very agreement between CrIS and IASI
- Line structure in CO (2155-2190 cm⁻¹) region provides very good information to retrieve CO amount, and line structure in CO₂ absorption band (2300-2370 cm⁻¹) provides very good spectral calibration information

CrIS Spectral Assessment: Cross-Correlation Method

- Two basic spectral validation methods are used to assess the CrIS SDR spectral accuracy
- Relative spectral validation, which uses two uniform observations to determine frequency offsets relative to each other
- Absolute spectral validation, which requires an accurate forward model to simulate the top of atmosphere radiance under clear conditions and correlates the simulation with the observed radiance to find the maximum correlation

Correlation coefficient between the two spectra:

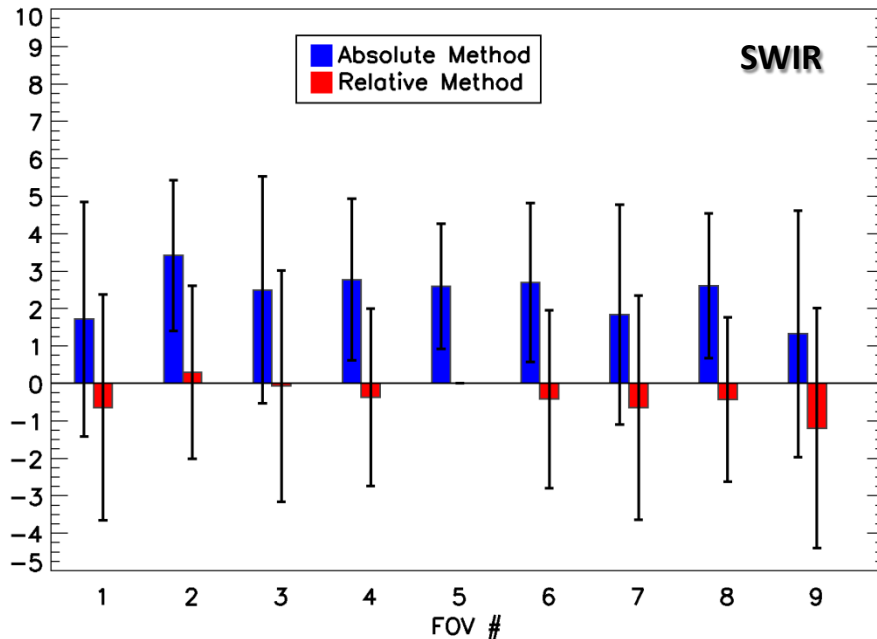
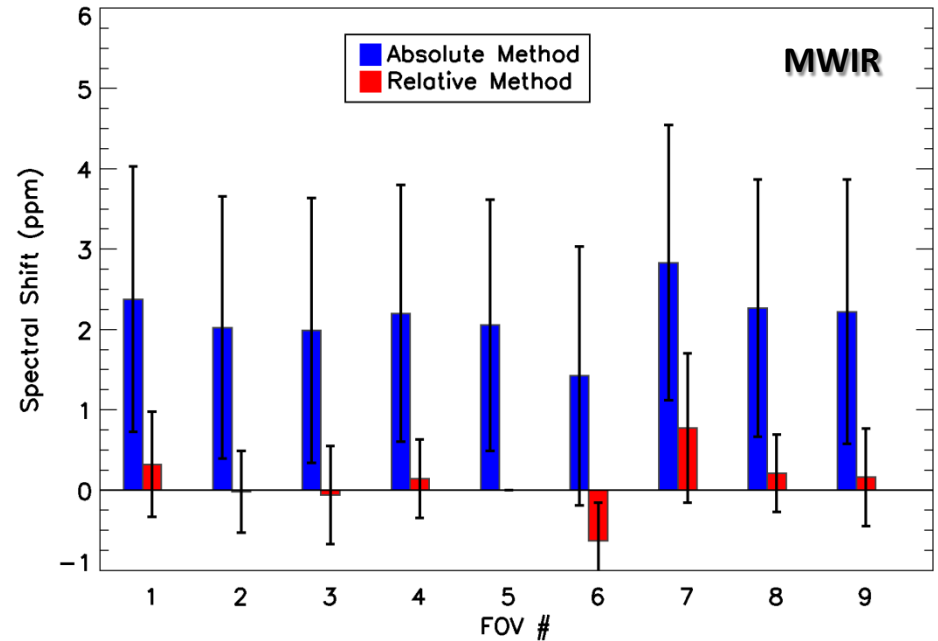
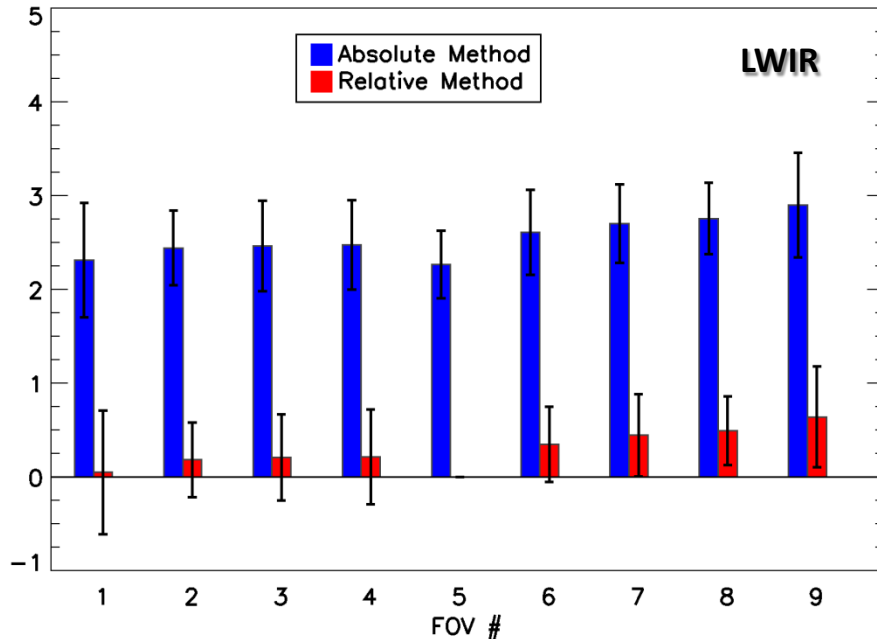
$$r_{S_1 S_2} = \frac{\sum_{i=1}^n (S_{1,i} - \bar{S}_1)(S_{2,i} - \bar{S}_2)}{(n-1)D_{S_1} D_{S_2}} = \frac{\sum_{i=1}^n (S_{1,i} - \bar{S}_1)(S_{2,i} - \bar{S}_2)}{\sqrt{\sum_{i=1}^n (S_{1,i} - \bar{S}_1)^2 (S_{2,i} - \bar{S}_2)^2}},$$

Standard deviation based on the difference of the two spectra:

$$D_{S_1 S_2} = \sqrt{\sum_{i=1}^n [(S_{1,i} - \bar{S}_1) - (S_{2,i} - \bar{S}_2)]^2} / (n-1).$$

The cross-correlation method is applied to a pair fine grid spectra to get the maximum correlation and minimum standard deviation by shifting one of the spectra in a given shift factor

CrIS Spectral Uncertainty



- Absolute cross-correlation method: between observations and CRTM simulations under clear sky over oceans to detect the spectral shift
- Relative method: observations from FOV 5 to other FOVs
- Frequency used: $710-760\text{ cm}^{-1}$, $1340-1390\text{ cm}^{-1}$, and $2310-2370\text{ cm}^{-1}$
- **Spectral shift relative to FOV5 are within 1 ppm**
- **Absolute spectral shift relative to CRTM within 3 ppm**

Summary

- ② The CrIS full resolution SDRs generated from the modified ADL were assessed
- ② Different calibration approaches are implemented in ADL to study the ringing
- ② CrIS full resolution SDR radiometric uncertainty:
 - FOV-2-FOV radiometric differences are small, within ± 0.3 K for all the channels
 - Double difference with IASI are within ± 0.3 K for most of channels
 - SNO results versus IASI show that agreement is very good for band 1 and band 2, but large BT differences in cold channels for band 3
- ② CrIS full resolution SDR spectral uncertainty:
 - Spectral shift relative to FOV5 are within 1 ppm
 - Absolute spectral shift relative to CRTM simulation are within 3 ppm